# Quantum structure of normal-liquid and supercritical $^4$He

K. A. Gernoth
*Institut für Theoretische Physik, Johannes Kepler Universität Linz, Altenbergerstrasse 69, A-4040 Linz, Austria and School of Physics and Astronomy, The University of Manchester, Manchester M13 9PL, United Kingdom*

M. Serhan
*Department of Physics, Al al-Bayt University, Jordan*

M. L. Ristig
*Institut für Theoretische Physik, Universität zu Köln, D-50937 Köln, Germany*

(Received 13 May 2008; revised manuscript received 25 July 2008; published 18 August 2008)

We study the temperature dependence of various spatial correlation functions of normal fluid and liquid $^4$He along an isochoric line of particle number density $\varrho=0.02185$ Å$^{-3}$. The formal and numerical investigation employs correlated density-matrix theory as currently developed. The formalism permits a clear analysis of particle exchange (statistical) effects and so-called direct-direct quantum effects that appear only in a many-body system of interacting particles. At supercritical temperatures $T\geq 12$ K the helium fluid can be characterized as a perfect quantum Boltzmann system. In such a fluid, quantum statistical correlations are absent and the particle exchange follows classical Boltzmann statistics despite direct-direct quantum effects being present. At temperatures below 12 K, statistical quantum correlations begin to appear and are largest at the Bose-Einstein transition temperature $T_{\mathrm{BE}}=2.17$ K. However, these correlations are considerably smaller than the statistical exchange correlations existing in a free Bose gas of bosons with helium mass. We present analytical and numerical results on the radial distribution function, the exchange correlation function, the phase-phase correlation function, the one-body reduced density matrix, and gross thermal quantities such as specific heat and total exchange energy. The role of particle exchange in determining their quantum properties is analyzed and discussed in detail.

DOI: 10.1103/PhysRevB.78.054513 PACS number(s): 61.20.−p, 67.25.−k, 67.10.Fj

## I. INTRODUCTION

Early theoretical investigations of quantum properties of fluid helium employed virial expansions and phase-shift analyses involving second- and third-order virial coefficients.[1,2] Reference 3 provides a comprehensive description of this theoretical and experimental work. Hill and Lounasmaa[4] measured and discussed quite a number of thermodynamic properties of fluid helium. Experimental data are also reported in Ref. 5 and by others.

The present theoretical analysis uses nonperturbative many-body theory that is applicable to strongly correlated quantum systems as well as to weakly interacting gases and charged systems. In this paper we study statistical and quantum properties of normal $^4$He along an isochore in the liquid phase as well as in the supercritical region of the fluid. The latter thermodynamic region is specified by the temperature and the particle density boundaries $T>T_c$ and $\varrho>\varrho_c$ to separate the low density gas region below the critical density $\varrho_c$ from the dense region of the system above the critical temperature $T_c$. For the helium system the critical point has the experimental values $\varrho_c=0.01$ Å$^{-3}$ and $T_c=5.2$ K. We report numerical results along the isochoric line $\varrho=0.02185$ Å$^{-3}$ in the temperature interval $T_{\mathrm{BE}}\leq T\leq 12$ K above the experimental transition temperature to the Bose-Einstein condensed states at $T_{\mathrm{BE}}=2.17$ K.

Complete information on these quantum properties is stored in the density matrix of the $N$-body system in question. However, the correlations of interest here are already contained in the reduced components. The diagonal elements of the reduced two-body density matrix provide the radial distribution function $g(r)$. Its Fourier transform yields the liquid structure function $S(k)$ that can be measured by suitable scattering experiments. The off-diagonal elements of the one-body reduced density matrix $n(r)$ constitute the Fourier inverse of the single-particle momentum distribution $n(k)$ which is also accessible experimentally. Related quantities are the kinetic energy distribution $\varepsilon_0(k)n(k)$ of the fluid, where $\varepsilon_0(k)=\hbar^2k^2/(2m)$, the total kinetic energy $E_{\mathrm{kin}}=\Sigma_{\mathbf{k}}\varepsilon_0(k)n(k)$ $(k=|\mathbf{k}|)$, etc. We analyze and evaluate these quantities and display their quantum structure.

The study builds upon a recent correlated density-matrix (CDM) analysis of the quantum structure existing in liquid parahydrogen.[6–9] This quantum liquid is well described as a perfect quantum Boltzmann liquid. For supercritical $^4$He at temperatures $T\geq 12$ K we find quite a similar behavior. However, in contrast to the $H_2$ liquid we may lower the temperature down to $T=2.17$ K, where helium condenses to the Bose-Einstein superfluid phase. For this reason we may experimentally and theoretically study the departure from Boltzmann statistics and the development of quantum statistical exchange correlations and their effect on various correlation functions and thermal quantities.

Within CDM theory the statistical effects of particle exchange are most clearly described by an appropriate quasiparticle picture. The formalism for correlated Bose fluids in their normal phases has been developed in Ref. 10. The quasiparticles are diagrammatically defined by so-called cyclic exchange (cc) diagrams. They determine the quasiparticle

 

momentum distribution $n_{qp}(k)$, the exchange correlation function $G_{cc}(r)$, the entropy of the system and therewith the specific heat.

These exchange correlations affect naturally the temperature dependence of the radial distribution function $g(r)$, the phase-phase correlations $P(r)$, the one-body reduced density matrix $n(r)$, and the related Fourier transforms $S(k)$, $P(k)$, and $n(k)$, respectively. Moreover, they influence the temperature dependence of the total kinetic energy, the exchange energy, etc. However, these quantities are strongly influenced by the quantum-mechanical so-called direct-direct (or dynamical) correlations directly induced by the strong particle-particle interaction potential. The interplay of exchange and dynamical properties is elucidated and discussed in detail in the following sections.

Section II collects the necessary formalism of CDM theory that displays the analytic structure of the correlation functions of interest that exists in a normal Bose fluid. It also provides the basic expressions and equations needed for numerical calculations by CDM theory. Section III focuses on the analytical and numerical results on the quantum statistical properties of normal fluid $^4$He. The screening of particle exchange in the radial distribution function $g(r)$ is then explored in Sec. IV. Section V reports and discusses the interplay between particle exchange and the direct-direct phase-phase correlations. Their combination determines the properties of the single-particle momentum distribution and the kinetic energy components of fluid $^4$He. A summary and brief outlook on future work is presented in Sec. VI. The Appendix lists the elementary contributions that are accounted for in the adopted hypernetted-chain (HNC)/4 approximation.

## II. STRUCTURAL ANALYSIS

We begin with a formal analysis of physical quantities expressing the microscopic structure of correlated Bose liquids and gases in their normal thermodynamic phase. CDM theory[10–12] provides an adequate and efficient tool for such an investigation. This formalism expresses the reduced density matrices characterizing a quantum system such as liquid or gaseous helium in an appropriate product form. The factors represent (i) particle exchange effects and (ii) direct-direct (or dynamical) effects directly induced by the particle interactions. A physical quantity of primary interest is the exchange (cc) correlation function $G_{cc}(r)$. Its factor decomposition is[6]

$$G_{cc}(r) = [1 + G_{dd}(r)]F_{cc}(r) \tag{1}$$

with the exchange component

$$F_{cc}(r) = \Gamma_{cc}(r) + N_{cc}(r) + E_{cc}(r). \tag{2}$$

The cyclic terms $\Gamma_{cc}(r)$, $N_{cc}(r)$, and $E_{cc}(r)$ are, respectively, the statistical input function, the nodal component, and the elementary portion of function (1). These functions are HNC components and are related by a set of HNC equations to direct-direct (dd) portions, direct-exchange (de) pieces, and exchange-exchange (ee) contributions defined in the CDM formalism. Explicit expressions and associated HNC equations are reported in Ref. 10.

The Fourier transforms $S_{cc}(k)$ and $\Gamma_{cc}(k)$ define the cyclic momentum distribution

$$n_{qp}(k) = \Gamma_{cc}(k)[1 + S_{cc}(k)] \tag{3}$$

within the quasiparticle concept of CDM theory.[10] These quasiparticles determine the entropy of the correlated boson fluid by the expression

$$S(T) = \sum_{\mathbf{k}} \{[1 + n_{qp}(k)]\ln[1 + n_{qp}(k)] - n_{qp}(k)\ln[n_{qp}(k)]\} \tag{4}$$

(ignoring the Debye spectrum of the collective excitations such as phonons). Consequently, these entities fix the theoretical temperature dependence of the specific heat.

In classical thermodynamics particles are completely distinguishable, thus statistical correlations do not exist, i.e., $G_{cc}(r)=0$ and $S_{cc}(k)=0$. In this case the distribution $\Gamma_{cc}(k)$ and its inverse Fourier transform $\Gamma_{cc}(r)$ are of the familiar Gaussian form. In quantum mechanics noninteracting identical bosons are indistinguishable and are therefore statistically strongly correlated. In this case the exchange structure function follows the equality $S_{cc}(k)=n_{qp}(k)$ and is represented by the familiar Bose function.

For normal fluid $^4$He and other strongly interacting boson systems the exchange structure function $S_{cc}(k)$ may differ very much from the two limiting cases just discussed, since strong repulsion between and among the particles prevents their exchange at short relative distances. These properties are explored in detail in Sec. III.

Equation (1) finds its counterpart in the product representation[6]

$$g(r) = [1 + G_{dd}(r)]F(r) \tag{5}$$

of the radial distribution function. The factor $F(r)$ embodies the effects of particle exchange and is of the explicit form

$$F(r) = F_{cc}^2(r) + [1 + N_{de}(r) + E_{de}(r)]^2 + N_{ee}(r) + E_{ee}(r). \tag{6}$$

The nodal ($N$) and elementary ($E$) pieces are defined in Ref. 10 and may be numerically evaluated by the HNC technique. The first factor in expression (5) takes account of the strong repulsion at short relative distances and therefore governs the degree of exchange screening existing in the spatial distribution $g(r)$. Section IV reports on this screening effect in liquid and supercritical $^4$He.

Inelastic neutron-scattering experiments allow to extract information on the momentum distribution $n(k)$ of a single particle in the fluid. It is therefore of great interest to analyze the quantum structure of this quantity and the concomitant kinetic energy distribution. CDM theory provides the genuine decomposition of the inverse Fourier transform $n(r)$ into its cyclic exchange factor $N_0(r)$ and the phase-phase (dd) correlation function $Q(r)$. The product reads[10,12]

$$n(r) = N_0(r)n_C \exp[-Q(r)]. \tag{7}$$

The exchange factor $N_0(r)$ is closely related to the quasiparticle distribution $n_{qp}(r)$. Its decomposition is therefore analogous to expression (2),

$$N_0(r) = \Gamma_{cc}(r) + N_{QQcc}(r) + E_{QQcc}(r). \quad (8)$$

The correlation function $Q(r)$ can be decomposed into a nodal component and an elementary portion,

$$Q(r) = N_{QQdd}(r) + E_{QQdd}(r). \quad (9)$$

It is shown in Refs. 12 and 10 that the nodal terms appearing in expressions (8) and (9) are factorizable in momentum space,

$$N_{QQcc}(k) = [1 + S_{cc}(k)][\Gamma_{cc}(k) + X_{Qcc}(k)]^2, \quad (10)$$

$$N_{QQdd}(k) = [X_{Qdd}(k) + X_{Qde}(k)][X_{Qdd}(k) + N_{Qdd}(k)] + X_{Qdd}(k)[X_{Qde}(k) + N_{Qde}(k)]. \quad (11)$$

Equations (10) and (11) permit a numerical evaluation by employing the HNC technique. The elementary terms in relations (8) and (9) are listed together with other elementary diagrams needed in the so-called HNC/4 approximation in the Appendix.

For a gas of noninteracting bosons function (7) specializes to $n(r)=N_0(r)=n_{qp}(r)$ and the quasiparticles are free particles characterized by the momentum distribution $n(k)=\Gamma_{cc}(k)[1-\Gamma_{cc}(k)]^{-1}$ with a statistical factor of Gaussian form. In the high-temperature limit $T\to\infty$ the distribution $n(k)$ is described by the classical Boltzmann expression $\Gamma_{cc}(k)=\varrho\lambda^3\exp[-\beta\varepsilon_0(k)]$ with the thermal wavelength $\lambda=(2\pi\beta\hbar^2/m)^{1/2}$.

In a strongly interacting fluid such as fluid $^4$He the statistical correlations can be dynamically suppressed and, therefore, the exchange quantities $N_0(r)$ and $n_{qp}(r)$ are still following Boltzmann statistics even at relatively low temperatures where dynamic quantum effects are already apparent. In normal $^4$He this situation occurs at temperatures $T\geq 12$ K. At $T=12$ K the quantum-mechanical phase-phase correlations described by function $Q(r)$ are already very large.

We note that the total number of quasiparticles in the normal bosonic phase is conserved and equals the total number $N$ of the ingredient particles. We therefore have the sum rules

$$n(r) = N_0(r) = n_{qp}(r) = 1 \quad \text{at} \quad r = 0 \quad (12)$$

and

$$Q(r=0) = \ln[n_C]. \quad (13)$$

Evidently, a boson system where the strength factor $n_C$ is unity does not correlate its phases at zero relative distances. However, due to the strong repulsion of the helium atoms fluid $^4$He develops large phase-phase correlations at distances $r\leq 2$ Å with $[-Q(r)]\geq 1$. Consequently, the strength factor $n_C$ is small, $n_C\ll 1$.

In addition to sum rules (12) and (13) we have a second-moment sum rule

$$-\frac{\hbar^2}{2m}[\nabla^2 n(r)]_{r=0} = E_{kin}/N \quad (14)$$

involving the one-body elements $n(r)$ and the total kinetic energy per particle, $E_{kin}/N$, of the fluid.

## III. QUANTUM STATISTICAL PROPERTIES

We employ the CDM formalism of Sec. II for a numerical study of the thermal and structural properties of fluid $^4$He at fixed particle number density $\varrho=0.02185$ Å$^{-3}$ in the temperature range $T_{BE}\leq T\leq 12$ K. Above these temperatures helium may be characterized by the absence of statistical correlations where the functions $G_{cc}(r)$ and $S_{cc}(k)$ are practically zero and the statistics of particles and quasiparticles is classical. Expressions (3), (5), and (8) read in this case

$$g(r) \approx 1 + G_{dd}(r) \quad (15)$$

and

$$n_{qp}(r) = N_0(r) = \Gamma_{cc}(r) = \exp[-\pi(r/\lambda)^2]. \quad (16)$$

The system displays therefore correlation effects only described by direct-direct dynamic diagrams contributing to functions $G_{dd}(r)$ and $Q(r)$. These statements are confirmed by the present numerical results within CDM theory. We stress that Eq. (16) does not hold for Bose systems where the screening of particle exchange is incomplete or completely absent as it is in the case of a system of noninteracting bosons. In a free Bose gas the particles are completely interchangeable in coordinate space and totally indistinguishable. For this system we still have the equality $n_{qp}(r)=N_0(r)$ for the one-body reduced density matrix or equivalently $n_{qp}(k)=N_0(k)$ for the corresponding Fourier transforms. However, in contrast to relation (16) the statistical factor $\Gamma_{cc}(r)$ differs from $n_{qp}(r)$. Free boson exchange instead leads to the Bose distribution $n_{qp}(k)=\Gamma_{cc}(k)[1-\Gamma_{cc}(k)]^{-1}$ with $\Gamma_{cc}(k)=\exp\{\beta[\mu_0-\varepsilon_0(k)]\}$ involving the associated chemical potential $\mu_0$. As a consequence, $n_{qp}(r)$ of free bosons exhibits quite a different behavior at large distances $r$ compared to the Gaussian dependence that exists in a system with perfect screening of particle exchange. For free bosons the asymptotic $r$-dependence is instead described by a Yukawa function[13] [cf. Eq. (16) therein]. We may see the differences in the ranges in Fig. 1. The dotted curve represents the one-body reduced density-matrix elements $n_{qp}(r)=G_{cc}(r)$ for a system of noninteracting $^4$He atoms at $T=4$ K. This should be compared with the result (full curve) that depicts function $G_{cc}(r)$ if the screening effect generated by the $^4$He–$^4$He interaction is included. This curve is of much shorter range than the one where the interparticle potential is switched off.

At temperatures in the range $T_{BE}\leq T\leq 12$ K the statistical properties depart from the classical Boltzmann description of the exchange functions $n_{qp}(r)$ and $N_0(r)$. The quantum statistical effects strongly influence the thermal behavior of the normal liquid phase of $^4$He and are largest at the phase transition temperature $T_{BE}=2.17$ K.

The present calculations are based on the HFDB2 Aziz interaction potential[14] and on adequate ansätze for the two input quantities which enter the set of HNC equations employed by CDM theory.[10] The so-called pseudopotential $u(r)$ that generates the dynamic correlations from the $^4$He–$^4$He potential is calculated from an Euler-Lagrange equation that optimizes the square root of the radial distribution function.

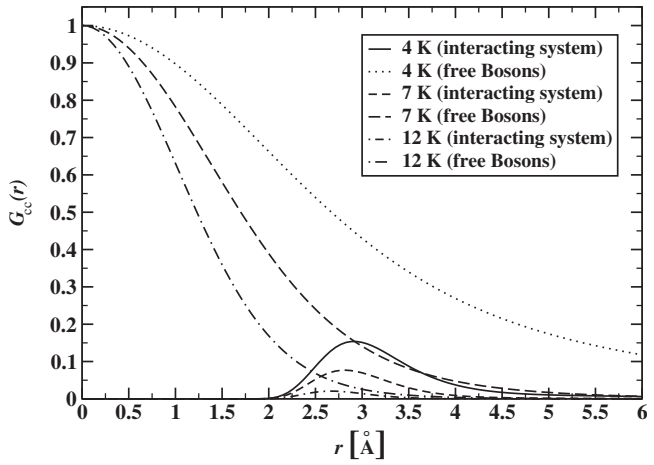


FIG. 1. Numerical results on the exchange correlation function $G_{cc}(r)$ of fluid $^4$He at three different temperatures. The CDM results are compared with the statistical correlations existing in a free gas of noninteracting helium atoms at the same temperatures and density. The comparison reveals the strong screening of particle exchange in fluid $^4$He due to the repulsion between the atoms at relative distances $r \leq 2$ Å. Note also the large difference between the correlation lengths at low temperature.

This optimization is by now a standard technique and phrased in terms of an effective Schrödinger equation with zero-energy eigenvalue.[6,15]

The input statistical factor $\Gamma_{cc}(k)$ may be cast in the general exponential form

$$\Gamma_{cc}(k) = \Gamma_{cc}(0)\exp[-\beta\varepsilon(k)] \tag{17}$$

with an energy $\varepsilon(k)=\hbar^2k^2/(2m^*)$. The effective mass $m^*$ represents the mass of a quasiparticle in the fluid and may, in general, depend on temperature and on momentum, $m^*=m^*(k,T)$.

In principle we may determine the effective mass by a strict functional optimization.[11] However, at present we adopt a simpler strategy. If the particles are entirely distinguishable, Boltzmann statistics would hold and the exact result for the effective mass would be $m^*(k,T)=m$. The same result would follow for free indistinguishable bosons.[10] Assuming the equality $m^*(k,T)=m$ for fluid/liquid $^4$He a CDM calculation at temperatures $T \geq 12$ K yields also very accurate results on various physical quantities in agreement with path-integral Monte Carlo (PIMC) simulation results.[8,9]

However, by retaining this assumption at low temperatures $T \leq 5$ K the corresponding CDM results yield an unrealistic theoretical Bose-Einstein temperature of about $T \approx 3.4$ K.[11] This deficiency stems from the fact that by assuming $m^*(k,T)=m$ the quantum statistical correlations embodied in the function $G_{cc}(r)$ are becoming too large in magnitude and range.

At present we therefore adopt the simple but reasonable ansatz for the effective mass

$$\frac{m^*(k,T)}{m} = \frac{1}{\alpha(T)} = 1 + \exp\left[1 - \frac{T}{T_{BE}}\right]. \tag{18}$$

Ansatz (18) neglects the possible dependence of the effective mass on wave number $k$. Its temperature dependence permits to find adequate physical solutions for the exchange structure function $S_{cc}(k)$ and the whole set of correlation functions and related quantities at all temperatures above the experimental temperature $T_{BE}=2.17$ K. No solutions of the CDM equations are found for the normal phase below this transition temperature. We may add some further arguments in support of ansatz (18). To arrive at this explicit and simple expression we performed a series of CDM calculations of the value of the statistical parameter $\Gamma_{cc}(0)$ appearing in Eq. (17) adopting the ansatz $\varepsilon(k)=\alpha\varepsilon_0(k)$. For any given value of the parameter $\alpha$ we have utilized sum rule (12) to evaluate the temperature dependence of the associated quantity $\Gamma_{cc}(0)$. The CDM calculations are performed at various temperatures but for temperature independent fixed values of $\alpha$ taken from the range $1 \geq \alpha \geq 1/2$. We then find a unique solution $\Gamma_{cc}(0)[T]$ for any given temperature $T$ above a certain limiting temperature $T_\alpha$. The value of this limiting temperature depends of course on the particular input datum for $\alpha$. No solutions for $\Gamma_{cc}(0)$ exist for $T<T_\alpha$. For the choice $\alpha=\frac{1}{2}$ the CDM calculation yields $T_\alpha=2.17$ K. If the value of the parameter $\alpha$ is increased we find an associated increase in the limiting temperature $T_\alpha$. For this reason we interpret the limiting case characterized by $\alpha=\frac{1}{2}$ as the signature for the transition from the normal phase to the superfluid phase and identify the associated $T_\alpha$ with the λ-transition temperature $T_{BE}=2.17$ K in liquid helium. At this temperature we have therefore $m^*/m=2$ in agreement with Eq. (18). At higher temperatures, $T>T_{BE}$, CDM theory then permits solutions for $\Gamma_{cc}(0)$ for smaller effective masses, $m^*<2m$. Assuming a monotonous decrease in $m^*(T)$ with increasing temperature allows therefore a smooth transition to the temperature region $T>12$ K, where the helium fluid is a perfect quantum Boltzmann system with $\alpha=1$ or equivalently $m^*=m$. The simple ansatz (18) reflects these properties quite naturally by adopting an exponential temperature dependence. To go beyond this heuristic approach in a strict systematic fashion one needs to develop a practical analytic optimization procedure and an appropriate numerical technique. We intend to develop these tools in the near future.

Numerical calculations within this realization of CDM theory are fast and efficient. Figure 1 displays numerical results on the exchange correlation function $G_{cc}(r)$ at three temperatures, $T=4$ K, $T=7$ K, and $T=12$ K at particle density $\varrho=0.02185$ Å$^{-3}$. These results are compared with analogous results on quantity $G_{cc}(r)$ but for a fluid of noninteracting helium atoms at same temperatures and density. We see a dramatic suppression of quantum statistical exchange correlations in the interacting helium fluid at distances $r \leq 2$ Å. The effect is caused by the hard-core repulsion between and among the atoms that keeps them distinguishable. Even at intermediate distances the magnitude and the range of the statistical correlation functions for $^4$He are distinctly smaller. Their maxima are located at about $r \approx 3$ Å where the helium potential is most attractive.

The amplitude decreases with increasing temperature and the correlations vanish in the supercritical $^4$He fluid at temperatures above 12 K. In this region the statistical factor $\Gamma_{cc}(r)$ is of the classical Gaussian form [Eq. (16)] and the particles are completely distinguishable.

Figure 2 displays the influence of the quasiparticle effective mass [Eq. (18)] on the size of the quantum statistical

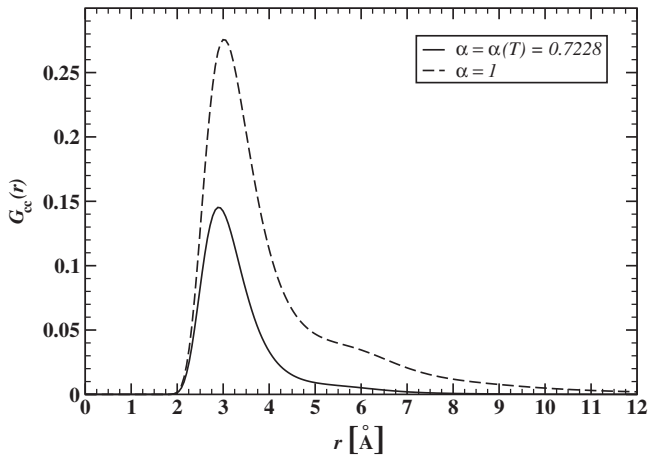


FIG. 2. The two curves display the effect caused by the effective mass $m^*(T)$ that increases with decreasing temperature in liquid $^4$He. The broken line represents CDM results on function $G_{cc}(r)$ if the mass is kept fixed at $m^*(T)=m$. The full line is the result where the temperature effect on $m^*(T)$ is taken into account ($T=4.5$ K and $m^*/m=1.384$).

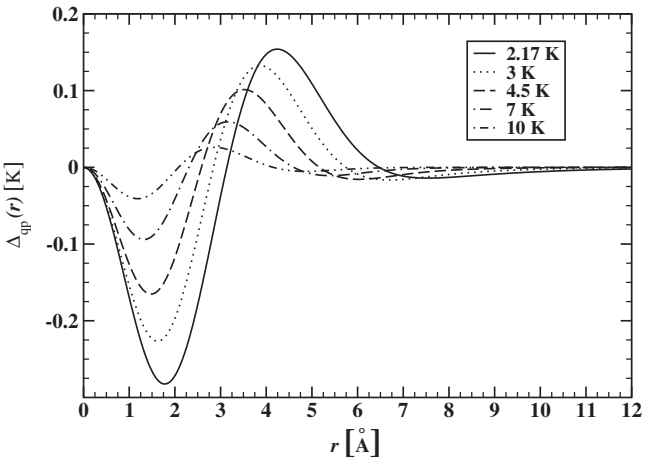


FIG. 3. Numerical results on function $\Delta_{qp}(r)$ of expression (19) within CDM theory that measures the quantum-mechanical departure from classical Boltzmann statistics in **r**-space experienced by the quasiparticles in liquid/fluid $^4$He. The quantum statistical effect decreases with increasing temperature and vanishes at about $T \approx 12$ K.

exchange. At $T=4.5$ K the effective mass is $m^*=1.384\ m$ leading to a correlation function $G_{cc}(r)$ with a maximum of about $G_{cc}(r\approx 3\ \text{Å})=0.15$ (full line). This result should be compared with the corresponding numerical data by CDM if we replace $m^*$ by the bare atomic mass $m$ at the same temperature (broken line). We observe that the effective mass $m^*$ causes an increased screening of the particle exchange reducing the magnitude and the range of the quantum statistical correlations. An important consequence of the temperature dependence of the effective mass [Eq. (18)] is therefore the lowering of the theoretical Bose-Einstein transition temperature to the value $T_{BE}=2.17$ K that very well agrees with the experimental result for liquid $^4$He.

The quantum properties of particle exchange are, evidently, reflected in the shape of the momentum distribution [Eq. (3)] and in the associated kinetic energy distribution $\varepsilon_0(k)n_{qp}(k)$ of the quasiparticles. At $T\geq 12$ K this distribution is of the familiar Maxwell-Gauß form and contributes an energy $\frac{3}{2}TN$ (Boltzmann constant $k_B=1$) to the total energy of the fluid. The departure from classical behavior at $T<12$ K is, of course, due to the quantum statistical correlations and may be measured by the difference

$$\Delta_{qp}(k) = \varepsilon_0(k)[n_{qp}(k) - n^B_{qp}(k)]. \tag{19}$$

The Boltzmann distribution $n^B_{qp}(k)$ is chosen such that the associated kinetic energy $\Sigma_{\mathbf{k}}\varepsilon_0(k)n^B_{qp}(k)$ equals the total quasiparticle energy

$$E_{qp} = \sum_{\mathbf{k}} \varepsilon_0(k)n_{qp}(k) \tag{20}$$

at same density and temperature.

This quantum-mechanical feature is also seen (Fig. 3) in the inverse Fourier transform $\Delta_{qp}(r)$. The shift from the classical to the quantum distribution in **r**-space is represented at five temperatures, $T=10$ K, 7 K, 4.5 K, 3 K, and at $T_{BE}=2.17$ K. In the supercritical region $T\geq 12$ K we have $\Delta_{qp}(r)\approx 0$. The quantum deviations increase with decreasing temperature. The difference $\Delta_{qp}(r)$ is negative in the repulsive range of the interaction and enlarged at intermediate distances.

Moreover, the temperature dependence of the effective mass [Eq. (18)] shapes the entropy [Eq. (4)] and therewith the specific heat of the normal $^4$He fluid and liquid. Figure 4 exhibits the CDM results on the specific heat at constant volume,

$$c_V(T) = \frac{T}{N}\left[\frac{\partial S(T)}{\partial T}\right]_V, \tag{21}$$

as a function of temperature (full line). The resulting curve approaches the classical constant $c_V(T)=3/2$ at large tem-

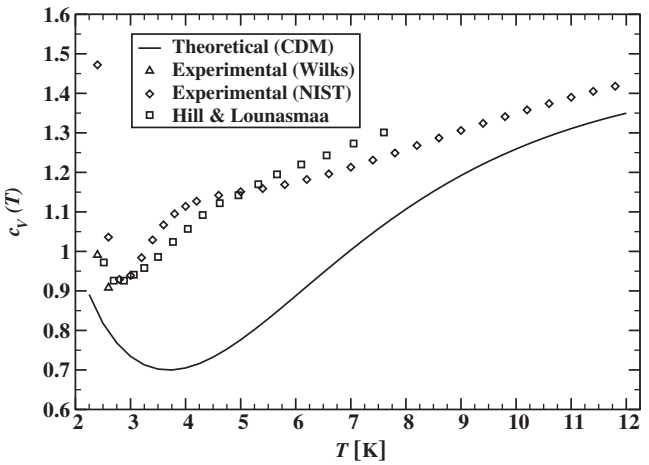


FIG. 4. CDM results on the specific heat per particle at constant volume carried by the quasiparticles with momentum distribution $n_{qp}(k)$. The theoretical results are compared with experimental data taken from Refs. 4, 5, and 16. The semiquantitative CDM results resemble the measured temperature dependence (see text for more comments).

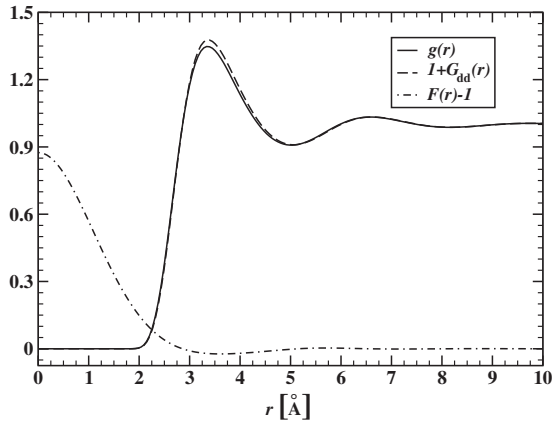


FIG. 5. Radial distribution function $g(r)$ of liquid $^4$He at $T=2.17$ K by CDM theory (full line). The dynamical (dd) component $1+G_{dd}(r)$ cuts off the particle exchange contributions. Only at temperatures $T$ close to the Bose-Einstein transition there is a very small area where the exchange function $F(r)-1$ overlaps with function $1+G_{dd}(r)$. This overlap leads to an insignificant slight reduction in the peak height of function $g(r)$. For temperatures $T \geq 4$ K the screening of particle exchange is complete.

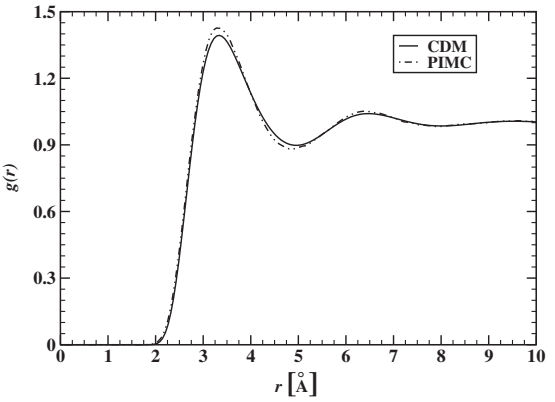


FIG. 6. Represented are numerical results on the radial distribution function $g(r)$ at $T=10$ K calculated by CDM in comparison with PIMC simulation data. As expected the Monte Carlo results show a little more shell structure than the CDM results that may be affected by the neglect of triplet correlations in the present realization of CDM theory.

peratures and decreases with decreasing temperature. At $T \approx 3.5$ K it reaches a minimum and rises again by further lowering of the temperature. This is in qualitative accordance with the experimental data on the heat capacity of liquid $^4$He and distinctively different from the monotonous temperature dependence of the specific heat of a free Bose gas. Our theoretical results are compared in Fig. 4 with experimental data reported by Hill and Lounasmaa,[4] Wilks,[5] and recent NIST data.[16] We suspect that the difference between the theoretical results on the specific heat and the experimental data may, in part, be due to the present neglect of contributions by collective excitations (phonons/rotons) which dominate in the superfluid phase but may possibly appear as remnants in the normal phase.

## IV. RADIAL DISTRIBUTION FUNCTION

The diagonal two-body reduced density-matrix elements $g(r)$ are a measure of the probability to find two atoms at a distance $r$ in fluid $^4$He. Due to the very strong repulsion between these atoms at distances $r \leq 2$ Å the radial distribution function [Eq. (5)] vanishes there. Thus, the exchange function $F(r)-1$ can only affect the dynamic component $G_{dd}(r)$ if its range exceeds the hard-core region.

In Fig. 5 we plot numerical results on functions $G_{dd}(r)$, $F(r)$, and the radial distribution function $g(r)$ at the lowest possible temperature $T=2.17$ K. Even at this temperature we find merely marginal differences between the CDM results for the radial distribution function and its direct-direct component $1+G_{dd}(r)$. We also display function $F(r)-1$ by CDM at the same temperature. Functions $1+G_{dd}(r)$ and $F(r)-1$ overlap only in the interval 2 Å $< r \leq 5$ Å with very small amplitude. The area of overlap decreases rapidly with increasing temperature. We may therefore conclude that particle exchange effects are practically absent from distribution $g(r)$ at all temperatures $T \geq 2.17$ K. Moreover, the very small exchange contributions in the normal liquid region of the $^4$He phase space (Fig. 5) will, presumably, be more than compensated by effects from triplet correlations[17] ignored in the present realization of CDM theory. This suggestion is supported by numerical results on the radial distribution function $g(r)$ of fluid $^4$He by PIMC (Refs. 18–20) calculations where triplet correlations are accounted for. Figure 6 shows numerical results by CDM on function $g(r)$ for supercritical $^4$He at $T=10$ K and density $\varrho=0.02185$ Å$^{-3}$ and compares them with data calculated by PIMC under same thermodynamic conditions. As expected, triplet correlations strengthen the correlated shell structure in contrast to the small effects generated by the exchange of $^4$He atoms that weakens the correlation structure of function $g(r)$.

At the present stage CDM theory does not incorporate three-body correlations which in comparison to the PIMC simulations is a drawback. The PIMC calculations automatically embody dynamical $n$-body correlations of any order $n$ and in this sense are exact for given interactions between the particles. However, the Fourier (or continuous imaginary time) path-integral Monte Carlo (FPIMC) method employed here and in earlier studies[6,18–20] uses Boltzmannon statistics that does not distinguish between bosons and fermions. Else, all other quantum-mechanical effects are fully taken into account in the FPIMC computations. CDM theory on the other hand can clearly distinguish between dynamical and quantum statistical correlations and contains the Bose statistics correctly, although with increasing temperature the quantum statistics is increasingly screened by the interparticle interactions. The neglect of quantum statistics in FPIMC becomes an issue at much lower temperatures than the one for which the comparison between FPIMC and CDM is shown in Figs. 6 and 7. At very low temperatures CDM has the advantage of incorporating the quantum statistical exchange correlations correctly. Discrete imaginary time PIMC (DPIMC) methods can be adapted to include Bose statistics.[21] More detailed discussions concerning the quantum statistics in FPIMC and discrete imaginary time PIMC may be found in Refs. 18–20.

A further issue concerning any computer simulation of physical systems, whether quantum or classical, FPIMC or

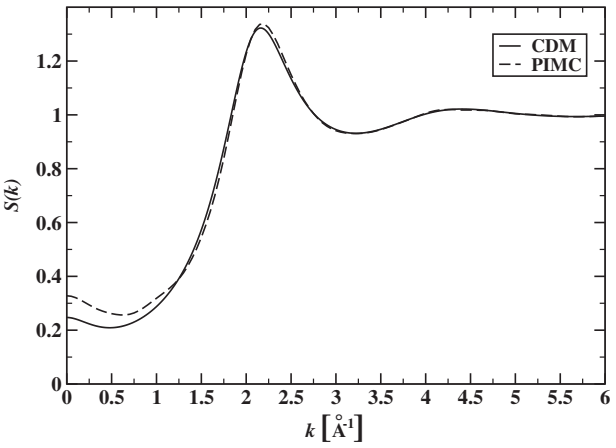


FIG. 7. Static liquid structure function $S(k)$ at $T=10$ K and at bulk particle number density $\varrho=0.02185$ Å$^{-3}$. The full curve displays the CDM result and the long-dashed curve the PIMC one (detailed discussion in text).

DPIMC, Monte Carlo or molecular dynamics, are finite-size effects due to the only finite number of particles in such simulations. In contrast to computational simulation procedures the thermodynamic limit is automatically built into the CDM method. The PIMC results shown here for $g(r)$ in Fig. 6 and $S(k)$ in Fig. 7 have been obtained with 384 particles, for which particle number the finite-size effects in $g(r)$ are already fairly small. Yet the finiteness of the simulated system still takes a vengeance when it comes to computing the liquid structure function $S(k)$ by means of the Fourier transform (FT) of the simulated $g(r)-1$. Because the maximum radial distance $r$ up to which the simulated $g(r)$ is computed is only 13.0402 Å the associated $S(k)$, when the $r$-integration to obtain $S(k)$ by means of the FT of $g(r)-1$ is simply cut off at that maximum value of $r$, is inaccurate for small $k$, although the location and height of the main peak agrees at $T=10$ K and $\varrho=0.02185$ Å$^{-3}$ reasonably well with the corresponding CDM result. This comparison between $S(k)$ from PIMC simulation and $S(k)$ from CDM is shown in Fig. 7 for $T=10$ K and $\varrho=0.02185$ Å$^{-3}$. Despite comparatively large differences between the two $S(k)$ for $k$ less than about 1.25 Å$^{-1}$ the agreement between the PIMC and the CDM $S(k)$ is still much better in the present case than for liquid parahydrogen at 16.5 K (cf. Fig. 4 in Ref. 6). We ascribe this to the fact that for the $^4$He systems considered here the spatial structure of the radial distribution function $g(r)$ is less pronounced and decays quicker as a function of $r$ than is the case for the $H_2$ systems treated in Ref. 6. A comparison between the PIMC and the CDM $^4$He $S(k)$ for $T=12$ K at the same density $\varrho=0.02185$ Å$^{-3}$ yields similarly good agreement, this agreement being even better for $k$ above about 1.25 Å$^{-1}$ in comparison to the situation at the lower temperature $T=10$ K. In case of liquid $H_2$ the PIMC $S(k)$ displays due to finite-size effects even an unphysical behavior and becomes negative for $k$ smaller than about 0.25 Å$^{-1}$ (cf. Ref. 6).

It must be said, however, that both in CDM theory as well as in Monte Carlo simulations it is the small-$k$ behavior of physical quantities that is notoriously difficult to compute accurately by means of the methods sketched above. This problem is reminiscent of experimental difficulties encountered at long wavelengths. In CDM these problems can be remedied much easier by simply extending the range of $r$ in the numerical programs, which can be done easily at hardly any mentionable expense in terms of CPU time, random access memory (RAM), or hard drive space. This is very different from the scaling behavior of computer simulations. Increasing the range of $r$ means an increase in the number of particles used in a simulation, which very quickly entails drastic increases in the demands on CPU time, RAM, and hard drive, the latter demand depending on which final results one opts to store for later use. Barring an ever further increase in the number of particles in simulations, one may alternatively resort to finite-size scaling methods or suitable extrapolations beyond the computed range to determine the long-range behavior in $r$-space and concomitantly the short-range behavior in $k$-space.

Speed of computation is clearly one of *the* major advantages of the CDM method. Due to the complexity of the CDM equations and the number of various quantities involved it indeed poses a programming challenge to develop a reliable numerical code that solves the CDM equations numerically. In the present applications the numerical CDM code typically runs by about a factor 1000 faster than the PIMC simulations. How much faster depends in the current situation mainly on the temperature. Whereas a CDM computation takes pretty much the same time regardless of temperature and density, FPIMC simulation time increases with decreasing temperature (and with decreasing particle mass and with increasing density), which is among other things due to the fact that at lower temperatures more points are needed in the FPIMC method to discretize continuous imaginary time on the interval [0,1] (see Refs. 18–20 for details). FPIMC simulation time scales linearly with the number of grid points used to represent continuous imaginary time. Furthermore, at present the FPIMC codes compute "only" energies and diagonal one- and two-body quantities[18–20] for solids and liquids alike but no other quantities such as the momentum distribution $n(k)$ or the spectrum of elementary excitations not to mention the host of other physical quantities that follow from CDM theory within a single coherent framework and that are all computed in one go.

To compare with available experimental results[22,23] for the liquid structure function $S(k)$ we have calculated the Fourier transform of the theoretical CDM results for the radial distribution function $g(r)$ at temperature $T=13.3$ K and density $\varrho=0.022$ Å$^{-3}$. The numerical results are shown in Fig. 8 (full curve). They may be compared with results of measurements performed under the same thermal conditions reported in Ref. 22 and displayed by the data in the middle of Fig. 1(a) therein. For comparison we have plotted in Fig. 8 some experimental data of this reference. They are indicated by crosses. Obviously, the theoretical and experimental results are in excellent agreement.

## V. KINETIC ENERGY COMPONENTS

In a classical many-body system each degree of freedom contributes an energy portion $T/2$ (in units of kelvin) to the

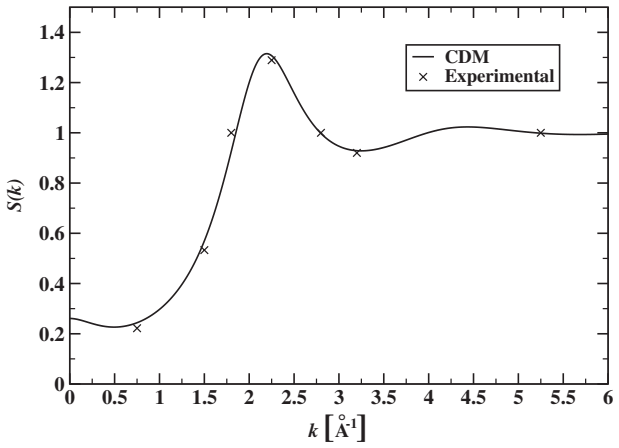


FIG. 8. Theoretical results on the liquid structure function $S(k)$ at temperature $T=13.3$ K and particle number density $\varrho=0.022$ Å$^{-3}$ for supercritical $^4$He by CDM. The crosses indicate the experimental results of Ref. 22 at selected wave numbers $k$ taken from Fig. 1(a) therein.

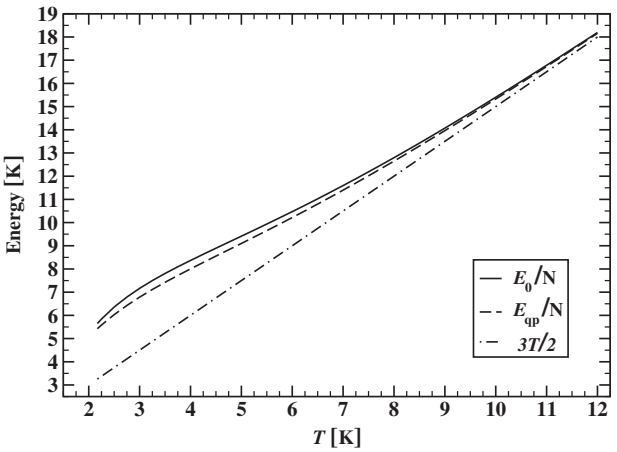


FIG. 9. Exchange energy $E_0/N$ of fluid $^4$He as function of temperature calculated by CDM (full line). At temperatures $T\geq 12$ K the results merge with the classical result $3T/2$ for the total kinetic energy per particle. The quantum corrections at temperatures $T<12$ K (difference between full and dot-dashed line) increase with decreasing temperature. At $T_{\mathrm{BE}}=2.17$ K they are of the same size as the classical portion. The broken line represents the CDM results for the kinetic energy of a quasiparticle, $E_{\mathrm{qp}}/N$. We see that the exchange energy is almost completely generated by the quasiparticles.

total energy. However, even at relatively high temperatures quantum correlations in fluid $^4$He produce a significant departure from the classical result $\frac{3}{2}TN$ for the total kinetic energy.

In CDM theory we may use the factor representation (7) to arrive at a decomposition of the energy expression (14) into an exchange component and a direct-direct quantum portion. The latter term is generated by the phase-phase dynamic correlations. The result is[6]

$$\frac{E_{\mathrm{kin}}}{N}=\frac{E_0}{N}+p_0\frac{E_p}{N}. \tag{22}$$

The first term represents the exchange energy per particle,

$$\frac{E_0}{N}=\frac{1}{N}\sum_{\mathbf{k}}\varepsilon_0(k)N_0(k)=-\frac{\hbar^2}{2m}[\nabla^2 N_0(r)]_{r=0}, \tag{23}$$

and the second term is the kinetic energy contribution generated by the direct-direct correlation function (9),

$$\frac{E_p}{N}=\frac{1}{N}\sum_{\mathbf{k}}\varepsilon_0(k)P(k)=-\frac{\hbar^2}{2m}[\nabla^2 P(r)]_{r=0}, \tag{24}$$

with the unit-normalized function $P(r)=Q(r)/Q(r=0)$. The value $|Q(r=0)|$ gives the strength factor $p_0=-\ln[n_C]$. In the high-temperature limit the energy [Eq. (23)] approaches the classical result. The quantum portion [Eq. (24)] has no classical analog.

In Fig. 9 we have plotted the CDM results on the exchange energy component [Eq. (23)] of normal helium as a function of temperature at density $\varrho=0.02185$ Å$^{-3}$ (full line). Lowering the temperature leads to a continuous increase of the quantum exchange part $E_0/N-\frac{3}{2}T$. At $T_{\mathrm{BE}}=2.17$ K we find a quantum energy of about 2.5 K added to the classical value $\frac{3}{2}T_{\mathrm{BE}}=3.26$ K. The kinetic energy of the quasiparticles defined by Eq. (20) almost coincides with the exchange kinetic energy $E_0$ at all temperatures (broken curve) thus indicating the close relationship between the distributions $n_{\mathrm{qp}}(k)$ and $N_0(k)$.

The relationship between the distributions can be also seen in the corresponding energy distributions $\varepsilon_0(k)n_{\mathrm{qp}}(k)$ and $\varepsilon_0(k)N_0(k)$ of the quasiparticles and the exchange energy distribution, respectively, of the $^4$He atoms in the fluid. Employing the analog of Eq. (19),

$$\Delta_0(k)=\varepsilon_0(k)[N_0(k)-N_0^{\mathrm{B}}(k)], \tag{25}$$

for measuring the departure of the exchange distribution $N_0(k)$ from its corresponding Maxwell distribution $N_0^{\mathrm{B}}(k)$ the CDM calculations reveal a dependence of expression (25) on wave number $k$ and temperature $T$ very similar to the results on function $\Delta_{\mathrm{qp}}(k)$. Figure 10 displays the quantum statistical properties of the one-body reduced density matrix [Eq. (7)] embodied in the measure [Eq. (25)]. The exchange quantity $\varepsilon_0(k)N_0(k)$ oscillates around the classical Maxwell distribution represented by $\Delta_0(k)=0$. The amplitude of the damped quantum oscillations decreases with increasing temperature. At $T=4.5$ K the magnitude is cut down by a factor of 0.5 from the value at $T=2.17$ K. The classical limit is reached in the supercritical region at $T\approx 12$ K as is the case for the quantum deviation $\Delta_{\mathrm{qp}}(k)$ of the quasiparticle energy distribution.

The quantum properties of the phase-phase correlations are embodied in the dd function $Q(r)$ and differ qualitatively and quantitatively from the exchange functions. The phase-phase correlations persist to much higher temperatures in contrast to the quantum exchange correlations. Numerical results on the unit-normalized function $P(r)=Q(r)/Q(0)$ are plotted in Fig. 11 at two temperatures. The numerical results

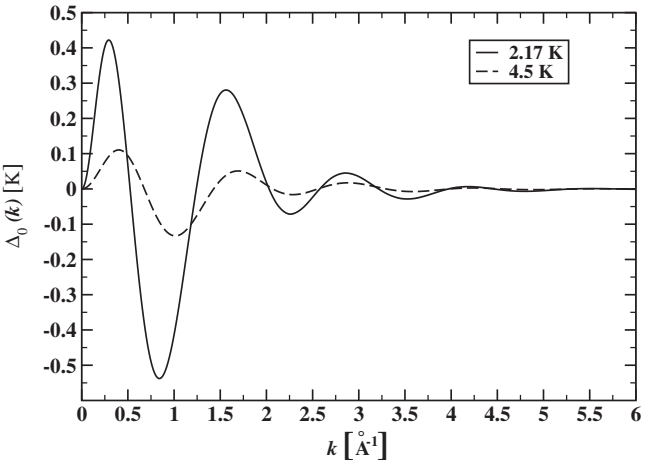


FIG. 10. CDM results on function $\Delta_0(k)$ that exhibits the quantum statistical effects contained in the exchange function $N_0(k)$ of a single $^4$He atom in the helium fluid. Quantum mechanics leads to damped oscillations about the corresponding classical Maxwell distribution $N_0^B(k)$. They have a correlation length of about 5 Å in the liquid phase and vanish in supercritical $^4$He.

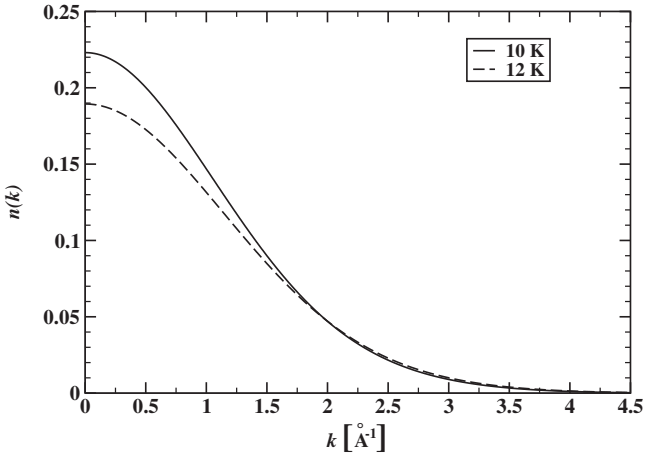


FIG. 12. Theoretical results on the momentum distribution $n(k)$ of fluid $^4$He at $T=10$ K and $T=12$ K. Despite that large phase-phase correlations exist at these and higher temperatures the momentum distribution is of classical Gaussian form, since the influence of the phase-phase correlations at fixed momentum $\hbar\mathbf{k}$ is small.

are almost independent of temperature at small values of $r$ and depend only weakly on temperature at distances 1 Å $<r<5$ Å. As a consequence, the phase-phase correlation energy [Eq. (24)] is still large at a temperature of $T=12$ K and at higher temperatures. CDM theory yields the energy component $p_0(E_p/N)=9.82$ K at $T=12$ K. This correlation energy decreases only slowly by a further increase in temperature. These properties of the phase-phase correlations in fluid $^4$He resemble very much the analogous properties studied theoretically and experimentally in liquid parahydrogen.[6,7]

We are now prepared to study the one-body reduced density matrix [Eq. (7)] with properties that are determined by the interplay of the exchange factor $N_0(r)$ with the phase-phase correlation function $Q(r)$. Employing the numerical results on both functions obtained by CDM theory we have calculated function $n(r)$ and its Fourier transform $n(k)$. Results on the momentum distribution $n(k)$ are displayed in Fig. 12 for fluid $^4$He at $T=10$ K and $T=12$ K and density $\varrho=0.02185$ Å$^{-3}$. At these temperatures the distribution $n(k)$ is very well represented by a classical Gaussian form despite the presence of large phase-phase correlations at this temperature. The property is documented by the results on the quantum measure

$$\Delta(k) = \varepsilon_0(k)[n(k) - n_B(k)] \tag{26}$$

for the momentum distribution $n(k)$ of the (true) particles. Expression (26) is the analog of the quantities $\Delta_{qp}(k)$ and $\Delta_0(k)$. The numerical results on measure $\Delta(k)$ for the helium system at temperatures 10 K and 12 K are shown in Fig. 13. We see a deviation from the classical distribution $\varepsilon_0(k)n_B(k)$ but its magnitude is very small. The maximum departure $|\Delta(k)|$ is only on the order of 0.05 K. This contrasts very much with the corresponding maximum values of $|\Delta_{qp}(k)|$ and $|\Delta_0(k)|$ being about ten times larger.

Comparing this finding with theoretical and experimental data on function (26) for liquid parahydrogen at $T=16.5$ K we see a large discrepancy between the small values $|\Delta(k)|$ for supercritical helium and corresponding values $|\Delta(k)|$ for liquid para$H_2$, $|\Delta(k)|\approx 0.4$ K (theory) and $|\Delta(k)|\approx 0.3$ K (experiment) at maximum (cf. Ref. 6, Fig. 9 therein).

The smallness of quantum measure (26) for fluid $^4$He may be explained by the larger atomic mass of the $^4$He atom compared to the mass of a $H_2$ molecule. This difference leads to a smaller thermal wavelength λ compared to the corresponding value of λ for $H_2$ at same temperature. It goes along with a shorter correlation length of the exchange function $N_0(r)$ in fluid $^4$He. Thus, the short-range exchange acts as a cut-off factor in the product [Eq. (7)]. It cuts off the relatively long-ranged phase-phase correlations in fluid $^4$He

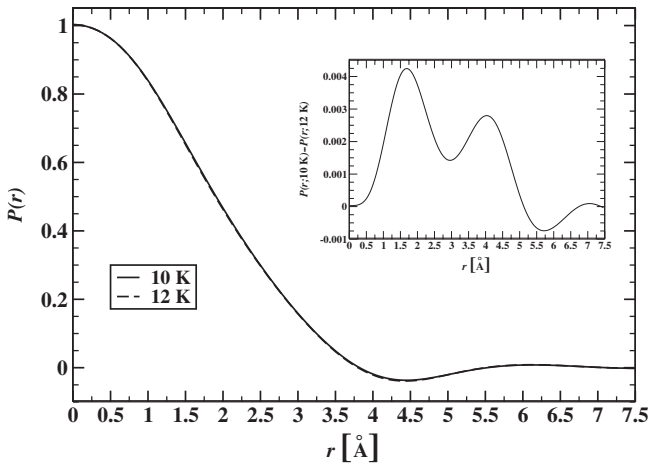


FIG. 11. The unit-normalized phase-phase correlation function $P(r)$ of fluid $^4$He by CDM. The curvature at small distances is practically independent of temperature in the entire range 2.17 K $\leq T\leq 12$ K considered. The very small differences between the results for $P(r)$ at $T=10$ K and $T=12$ K are displayed in the inserted diagram.

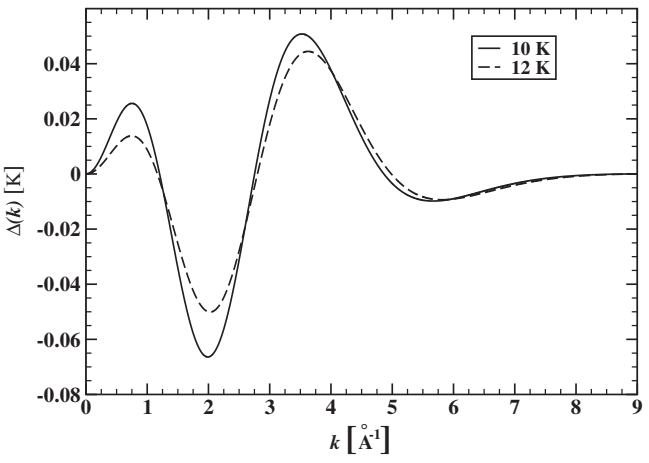


FIG. 13. CDM results on function $\Delta(k)$, Eq. (26), that measures the influence of quantum effects on the kinetic energy distribution $\varepsilon_0(k)n(k)$ in supercritical $^4$He at $T=10$ K and $T=12$ K. At these temperatures exchange correlations between the constituents are entirely absent and the magnitude of the phase-phase correlations is very small.

and reduces therefore the "quantumness" of function $n(r)$ and the momentum distribution $n(k)$. We mention that experimental measurements on function $n(k)$ are presently under way to analyze these quantum properties of fluid and liquid $^4$He.

## VI. SUMMARY AND OUTLOOK

We have presented a detailed theoretical investigation of the quantum structure of liquid and supercritical $^4$He as a function of temperature. The study emphasizes the particular role of quantum statistical correlations that originates in the strongly repulsive $^4$He$-^4$He interaction at short interparticle distances. The analysis employs correlated density-matrix theory providing the appropriate method of choice.

Noninteracting bosons are characterized by strong quantum-mechanical statistical correlations due to their indistinguishability. However, in the helium system these exchange correlations are very much suppressed and are nonzero only at intermediate interparticle distances. They increase, however, if the temperature is lowered. This increase is controlled by an appropriate temperature dependence of an effective mass. The temperature dependence of this mass determines the location of the Bose-Einstein transition temperature and the shape of the specific heat curve at constant volume.

The quantum statistical effects fall off in the supercritical phase region of fluid $^4$He around a temperature $T\approx 12$ K and the system can be characterized as a quantum Boltzmann fluid. We further studied the effects of statistical correlations on the behavior of the one-body reduced density matrix $n(r)$ and the diagonal two-body reduced matrix elements $g(r)$. CDM theory reveals that the particle exchange is very much suppressed in the entire temperature range of normal helium. Only very close to the transition temperature $T_{\mathrm{BE}}$ one finds very small deviations of $g(r)$ from the dynamic component $1+G_{\mathrm{dd}}(r)$. The liquid structure function $S(k)$, which follows from the Fourier transform of $g(r)$, is therefore not affected by exchange correlations.

The momentum distribution and the kinetic energy distribution in **k**-space have been decomposed into statistical components and dynamic portions. The first component is characterized by the distribution $N_0(k)$, the latter one by the phase-phase correlation function $P(r)$ or $Q(r)$. The exchange function $N_0(k)$ has many features in common with the quasiparticle momentum distribution $n_{\mathrm{qp}}(k)$. Both functions depart from the classical Boltzmann behavior at temperatures $T\leq 12$ K. The dynamic effects embodied in the correlation function $Q(r)$ in $^4$He do not exist in classical many-body systems, since they characterize the off-diagonal elements of the density matrix. In fluid $^4$He this quantum contribution persists to rather high temperatures exceeding 12 K and its large strength $p_0$ could be experimentally detected.

The numerical results are derived by CDM in the so-called HNC/4 approximation. The HNC summation technique has been exploited with great success for studying the correlated ground and excited states at zero temperatures within correlated basis functions (CBF) theory.[24] The generalization to nonzero temperature takes account of the contributions described by a set of exchange diagrams.[10,25] The HNC/4 approximation includes all dynamic and exchange diagrams which can be constructed by series and parallel connections from basic elements involving renormalized elementary four-point diagrams.

The present study does not include contributions from triplet correlations generated by a three-body pseudopotential[17] and/or by a three-body statistical exchange factor.[15] If desired for a more sophisticated investigation of specific effects the CDM formalism can be carried (at least in principle) to the next level of approximation within a systematic formal procedure.

However, in our opinion, it would at present be of prior interest to (i) apply CDM theory to other interesting quantum systems such as liquid deuterium and $\alpha$-matter. The latter boson system is studied in nuclear physics;[26] (ii) generalize the CDM approach for application to the Bose-Einstein condensed phase of liquid $^4$He,[25] and perform neutron-scattering experiments on liquid and supercritical $^4$He to measure the momentum distribution and other physical quantities of interest along isochoric lines or along an isotherm to compare with here presented theoretical results at same temperatures and densities.

## ACKNOWLEDGMENTS

We are particularly indebted to E. Krotscheck for his help with the numerical procedure to evaluate elementary diagrams numerically. One of us (M.S.) thanks the Deutscher Akademischer Austauschdienst (DAAD) for financial support of his research work at the Universität zu Köln.

## APPENDIX: ELEMENTARY FOUR-POINT DIAGRAMS

The HNC/4 approximation includes the contributions of a complete set of elementary diagrams with four field points

within the HNC classification scheme. These components are $E_{dd}(r)$, $E_{de}(r)$, $E_{ee}(r)$, $E_{cc}(r)$, $E_{Qdd}(r)$, $E_{Qde}(r)$, $E_{Qcc}(r)$, $E_{QQdd}(r)$, and $E_{QQcc}(r)$. They may be characterized by generalized Ursell-Mayer diagrams[12,25] representing the following double integrals over the entire volumes $V$:

$$E_{Qdd}(r) = \frac{1}{2}\varrho^2 \int G_{dd}(r_{13})G_{dd}(r_{14})G_{Qdd}(r_{23})G_{Qdd}(r_{24}) \times [G_{dd}(r_{34}) + G_{ee}(r_{34})]d\mathbf{r}_3 d\mathbf{r}_4, \quad \text{(A1)}$$

$$E_{Qde}(r) = \varrho^2 \int G_{Qdd}(r_{23})G_{Qdd}(r_{24}) \times [G_{ee}(r_{13})G_{dd}(r_{14})G_{dd}(r_{34}) + G_{cc}(r_{13})G_{cc}(r_{14})G_{cc}(r_{34})]d\mathbf{r}_3 d\mathbf{r}_4, \quad \text{(A2)}$$

$$E_{Qcc}(r) = \varrho^2 \int G_{Qdd}(r_{23})G_{Qcc}(r_{24}) \times [G_{cc}(r_{13})G_{dd}(r_{14})G_{cc}(r_{34}) + G_{dd}(r_{13})G_{cc}(r_{14})G_{dd}(r_{34})]d\mathbf{r}_3 d\mathbf{r}_4, \quad \text{(A3)}$$

$$E_{QQdd}(r) = \frac{1}{2}\varrho^2 \int G_{Qdd}(r_{13})G_{Qdd}(r_{23})G_{Qdd}(r_{14})G_{Qdd}(r_{24}) \times [G_{dd}(r_{34}) + G_{ee}(r_{34})]d\mathbf{r}_3 d\mathbf{r}_4, \quad \text{(A4)}$$

$$E_{QQcc}(r) = \varrho^2 \int G_{Qdd}(r_{23})G_{Qcc}(r_{24}) \times [G_{Qdd}(r_{14})G_{Qcc}(r_{13})G_{cc}(r_{34}) + G_{Qcc}(r_{14})G_{Qdd}(r_{13})G_{dd}(r_{34})]d\mathbf{r}_3 d\mathbf{r}_4, \quad \text{(A5)}$$

$$E_{ee}(r) = \varrho^2 \int G_{dd}(r_{34})[G_{dd}(r_{14})G_{dd}(r_{23})G_{ee}(r_{13})G_{ee}(r_{24}) + G_{cc}(r_{14})G_{cc}(r_{23})G_{cc}(r_{13})G_{cc}(r_{24})]d\mathbf{r}_3 d\mathbf{r}_4. \quad \text{(A6)}$$

Omission of the subscripts $Q$ in Eqs. (A1)–(A3) yields the explicit expressions for the elementary components $E_{dd}(r)$, $E_{de}(r)$, and $E_{ee}(r)$, respectively.

We rescale the elementary components $E_{QQcc}$ and $E_{QQdd}$ by the replacements $\alpha_c E_{QQcc}$ and $\alpha_d E_{QQdd}$, respectively. The scaling factors $\alpha_c$ and $\alpha_d$ are chosen such that the sum rule $N_0(r=0)=1$ and the kinetic energy rule [Eq. (14)] with $E_{kin}/N$ calculated by PIMC simulation are exactly fulfilled.


[1] J. E. Kilpatrick, W. E. Keller, E. F. Hammel, and N. Metropolis, Phys. Rev. **94**, 1103 (1954).
[2] S. Y. Larsen, K. Witte, and J. E. Kilpatrick, J. Chem. Phys. **44**, 213 (1966).
[3] W. E. Keller, *Helium-3 and Helium-4* (Plenum, New York, 1969).
[4] R. W. Hill and O. V. Lounasmaa, Philos. Trans. R. Soc. London, Ser. A **252**, 357 (1960).
[5] J. Wilks, *The Properties of Liquid and Solid Helium* (Clarendon, Oxford, 1967).
[6] K. A. Gernoth, T. Lindenau, and M. L. Ristig, Phys. Rev. B **75**, 174204 (2007).
[7] J. Dawidowski, F. J. Bermejo, M. L. Ristig, C. Cabrillo, and S. M. Bennington, Phys. Rev. B **73**, 144203 (2006).
[8] K. A. Gernoth, M. L. Ristig, and T. Lindenau, Int. J. Mod. Phys. A **21**, 257 (2007).
[9] K. A. Gernoth, M. L. Ristig, and T. Lindenau, in *Condensed Matter Theories*, edited by H. Reinholz, G. Röpke, and M. de Llano (World Scientific, Singapore, 2007), Vol. 22.
[10] G. Senger, M. L. Ristig, C. E. Campbell, and J. W. Clark, Ann. Phys. (N.Y.) **218**, 160 (1992).
[11] M. L. Ristig, T. Lindenau, M. Serhan, and J. W. Clark, J. Low Temp. Phys. **114**, 317 (1999).
[12] R. Pantförder, T. Lindenau, and M. L. Ristig, J. Low Temp. Phys. **108**, 245 (1997).
[13] M. Luban and M. Revzen, J. Math. Phys. **9**, 347 (1968).
[14] R. A. Aziz, M. J. Slaman, A. Koide, A. R. Allnat, and W. J. Meath, Mol. Phys. **77**, 321 (1992).
[15] G. Senger, M. L. Ristig, K. E. Kürten, and C. E. Campbell, Phys. Rev. B **33**, 7562 (1986).
[16] E. W. Lemmon, M. O. McLinden, and D. G. Friend, in *NIST Chemistry WebBook*, NIST Standard Reference Database No. 69, edited by P. J. Linstrom and W. G. Mallard (National Institute of Standards and Technology, Gaithersburg, MD, 2005), http://webbook.nist.gov
[17] C. E. Campbell, Phys. Lett. **44A**, 471 (1973).
[18] K. A. Gernoth, Ann. Phys. (N.Y.) **285**, 61 (2000).
[19] K. A. Gernoth, Ann. Phys. (N.Y.) **291**, 202 (2001).
[20] K. A. Gernoth, Z. Kristallogr. **218**, 651 (2003).
[21] D. M. Ceperley, Rev. Mod. Phys. **67**, 279 (1995).
[22] W. Montfrooij, L. A. de Graaft, P. J. van den Bosch, A. K. Soper, and W. S. Howells, J. Phys.: Condens. Matter **3**, 4089 (1991).
[23] R. M. Crevecoeur, H. E. Smorenburg, and I. M. de Schepper, J. Low Temp. Phys. **103**, 313 (1996).
[24] E. Feenberg, *Theory of Quantum Fluids* (Academic, New York, 1969).
[25] M. L. Ristig, G. Senger, M. Serhan, and J. W. Clark, Ann. Phys. (N.Y.) **243**, 247 (1995).
[26] G. Röpke and P. Schuck, Mod. Phys. Lett. A **21**, 2513 (2006).